Journal of Sound and Vibration (1982) **84**(1), 57–79

A METHOD FOR MODAL IDENTIFICATION OF LIGHTLY DAMPED STRUCTURES

D. J. EWINS

Department of Mechanical Engineering, Imperial College of Science and Technology, London SW7 2BX, England

AND

P. T. GLEESON

Department of Science and Mathematics, Middlesex Polytechnic, London N11 2NQ, England

(*Received* 1 *May* 1981, *and in revised form* 29 *December* 1981)

In many cases modal tests are conducted on individual components of complex engineering structures where interest is confined to deriving an undamped model of the structure. A method is proposed for this task which demands a minimum of input data and which, in particular, does not require accurate measurements around resonance. The method is simple to program and its application to various practical structures is described.

1. INTRODUCTION

Experimental modal analysis, or vibration system identification, has become an increasingly popular technique in recent years. Developments in measurement and instrumentation technology have facilitated the acquisition of data of sufficient accuracy to be submitted to the calculation procedures which constitute modal analysis, leading to extraction of the modal properties of a test structure, and thence to a mass and stiffness model of it.

One of the earliest such techniques used on mechanical structures was that of Salter [1] based on a graphical analysis, and we shall return to his work later.

However, the recent development of numerical modal analysis algorithms has been extensive and the curve-fitting procedures upon which they are based are very refined [2, 3]. These methods are generally proven by using synthesized data, usually polluted with random errors to add realism, and in these test cases they perform excellently. However, their very refinement can render them remote from their users who will often not appreciate the finer aspects of their workings, nor know how to proceed following an unsatisfactory result. In this paper and its companion [4], the use of modal analysis techniques for practical applications is examined and two complementary and simple methods are presented which can be programmed with relative facility on either mini- or mainframe computers.

This present paper is concerned with a class of structures whose demands on the modal analysis process are essentially for a simple undamped model. Such is the case when the damping in the test structure is both relatively small (thereby permitting the following method to be used) and of no intrinsic interest (so that its exclusion from the analysis process is of no consequence). This situation is encountered in a great many practical applications, and especially those which include studies and modelling of the individual

0022-460X/82/170057+23 $03.00/0

components which form part of an assembled structure. Usually, the individual components are themselves very lightly damped, and such damping as they do possess is often of little consequence to the assembled structure which generally derives most of its damping from the junctions and joints between the various components. Also, interest is generally confined in these studies to predicting the natural frequencies of the assembly from knowledge of its components, and for this purpose the damping is unimportant. These premises are very similar to those of Salter [1].

In addition to providing a simple means for analyzing virtually undamped structures, the method described below is also useful as an alternative to the more common curve-fitting procedures, such as that described in reference [4], which rely heavily on frequency response measurements near resonance. Under certain conditions, these resonance data will be ill defined or inaccurate due to measurement problems or to non-linear behaviour of the structure, and in such cases, the method described below can provide a valuable means of avoiding serious errors in the modelling procedure.

Although quite different in its method of use, the procedure described below does exhibit marked similarities to the graphical method of Salter [1], the general shape of the frequency response curve rather than detailed measurements in resonant regions being used in both. It is based upon the fact that the locations of resonance and antiresonance frequencies are determined by the mass and stiffness properties of the structure.

2. THEORETICAL BASIS

2.1. MATHEMATICAL FOUNDATION OF MODAL ANALYSIS

The response $q_j(\omega)$ to an input force $Q_k(\omega)$ of a harmonically excited N-degree-of-freedom system with hysteretic damping may be expressed in modal terms as a receptance,

$$\alpha_{jk}(\omega)=\frac{q_j(\omega)}{Q_k(\omega)}=\sum_{r=1}^{N}\frac{({}_r\phi_j)({}_r\phi_k)}{(\lambda_r^2-\omega^2)}, \tag{1}$$

where ${}_r\phi_j$ is the jth element of the rth complex mode shape vector $\{\phi\}_r$. One may define a "modal constant" ${}_rA_{jk}$ as

$${}_rA_{jk}={}_r\phi_j\,{}_r\phi_k, \tag{2}$$

and obtain the equation

$$\alpha_{jk}(\omega)=\sum_{r=1}^{N}\frac{{}_rA_{jk}}{(\lambda_r^2-\omega^2)}. \tag{3}$$

In this form the equation is identical to equation (9.5.14) quoted by Bishop and Johnson [5].

It is convenient to write the complex quantity λ_r^2 as:

$$\lambda_r^2=\omega_r^2(1+\mathrm{i}\eta_r), \tag{4}$$

where ω_r is the natural frequency and η_r the loss factor of the rth mode. The receptance $\alpha_{jk}(\omega)$ may thus be rewritten as

$$\alpha_{jk}(\omega)=\sum_{r=1}^{N}\frac{{}_rA_{jk}}{\omega_r^2[1-(\omega/\omega_r)^2+\mathrm{i}\eta_r]}. \tag{5}$$

The corresponding inertance $I_{jk}(\omega)$ may be written as

$$I_{jk}(\omega)=\frac{\ddot{q}_j(\omega)}{Q_R(\omega)}=-\omega^2\alpha_{jk}(\omega)=\sum_{r=1}^{N}\frac{{}_rA_{jk}}{1-(\omega_r/\omega)^2(1+i\eta_r)}. \tag{6}$$

Inertance data are available directly from practical measurements with accelerometers and force transducers.

2.2. IDENTIFICATION OF MODAL CONSTANTS FROM MEASURED INERTANCES

For a system with negligible damping, equation (6) may be written as

$$I_{jk}(\omega)=\sum_{r=1}^{N}\frac{{}_rA_{jk}}{1-(\omega_r/\omega)^2}. \tag{7}$$

One can select N discrete response frequencies $\Omega_1, \Omega_2, \ldots, \Omega_N$ and incorporate the corresponding inertances into a matrix equation:

$$\begin{Bmatrix} I_{jk}(\Omega_1) \\ I_{jk}(\Omega_2) \\ \vdots \\ I_{jk}(\Omega_N) \end{Bmatrix} = \begin{bmatrix} (1-\omega_1^2/\Omega_1^2)^{-1} & (1-\omega_2^2/\Omega_1^2)^{-1} & \cdots \\ \vdots & \vdots & \\ (1-\omega_1^2/\Omega_N^2)^{-1} & \cdots & (1-\omega_N^2/\Omega_N^2)^{-1} \end{bmatrix} \begin{Bmatrix} {}_1A_{jk} \\ {}_2A_{jk} \\ \vdots \\ {}_NA_{jk} \end{Bmatrix},$$

or

$$\{I_{jk}(\omega)\}_{N\times 1}=[R]_{N\times N}\{A_{jk}\}_{N\times 1}, \tag{8}$$

always provided that no selected response frequency may coincide with a natural frequency.

The matrix $[R]$ contains terms which are functions only of the natural frequencies and the selected response frequencies. The terms are real and of either sign and the matrix is very easy to invert with negligible error, thus allowing the identification of modal constants in terms of response data:

$$\{A_{jk}\}=[R]^{-1}\{I_{jk}(\omega)\}. \tag{9}$$

2.3. DAMPING

Sometimes it is convenient to include a modal loss factor as a secondary correction if inclusion of approximate damping terms is thought to be necessary. The simplest approach is found by considering equation (5) for the condition $\omega=\omega_r$. In this case, for sufficiently light damping, the series for $\alpha_{jk}(\omega_r)$ is dominated by the rth term and there is a resonance peak whose amplitude has negligible contributions from other modes. The equation is

$$\hat{\alpha}_{jk}(\omega_r)={}_rA_{jk}/i\eta_r\omega_r^2, \tag{10}$$

from which the loss factor is obtained as

$$\eta_r=|{}_rA_{jk}|/|\hat{\alpha}_{jk}(\omega_r)|\omega_r^2. \tag{11}$$

This formulation has been given by Ewins [6] who developed it further to obtain the loss factor in terms of measured responses at two near-resonance frequencies.

3. IMPLEMENTATION OF IDENTIFICATION PROCEDURE

3.1. COMPUTER PROGRAM

A computer program has been written to carry out the calculations outlined in the foregoing sections. The "standard" way of using the program is as follows: first, to plot the frequency response corresponding to a set of measured data read from file or tape; second, to set up matrix $[R]_{N\times N}$ and vector $\{I\}_{N\times 1}$ of selected measured data and to solve by matrix inversion to give $[R]^{-1}$ and the vector $\{A\}$ of modal constants (the damping loss factor can be estimated from near-resonance response data if required); third, to regenerate the response from the modal constants and to compare this with the original by plotting it on the same graph, preferably with use of continuous lines in contrast to the discrete points of measured values. If the comparison is not sufficiently close, another selection of response data may be made and the second and third steps repeated.

3.2. SELECTION OF DATA POINTS

Although very simple in concept, the success of the method in practical situations depends upon the choice of the very few data required as input and this topic is discussed in some detail.

3.2.1. *Complete modal representation*

The frequency response of an undamped single mode is shown in Figure 1 as a logarithmic plot of mobility modulus versus frequency. The symmetry about the vertical asymptote is a convenient feature of mobility $(\dot{q}(\omega)/Q(\omega))$ as distinct from receptance or inertance, whose plots are skewed.

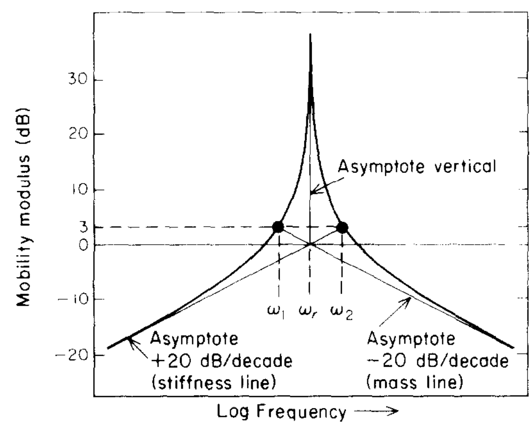

Figure 1. The frequency response of a single mode. 0 dB corresponds to A_r/ω_r; $\omega_1 = \omega_r/\sqrt{2}$; $\omega_2 = \omega_r \times \sqrt{2}$.

When several modes with modal constants of differing magnitudes are combined, the resultant mobility plot will be as in Figure 2, which illustrates a 4-mode system. The signs on the curve segments indicate the phase of the corresponding mobility: i.e., +90° or −90°.

The identification calculation of equation (9) requires knowledge of the four natural frequencies ω_1 to ω_4 and of the frequency response data at the four selected response frequencies Ω_1 to Ω_4. The mobilities Y_1 to Y_4 are readily transformed into inertances of correct sign for inclusion in the equation. The selection of four from the many responses for which data would be available from a mobility measurement can be quite arbitrary in this case of complete modal representation. The response curve can be regenerated from the set of four identified modal constants by using equation (7) for a large number of values of ω. This regenerated curve will coincide with the original response data within

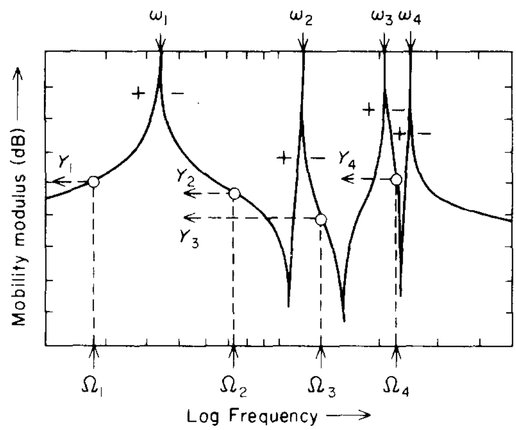

Figure 2. Selection of response data for identification: complete modal representation.

a close tolerance which is directly related to the error in measurement of inertance or mobility.

3.2.2. *Incomplete modal representation*

In the majority of practical cases, vibration data are acquired by measurement over limited frequency ranges on structures which, being continuous, have a great many degrees of freedom and a corresponding number of modes. Thus it is generally impossible to carry out complete modal analysis which encompasses all the modes, and in the general case an N-mode representation has to be used to approximate to a greater-than-N set of data.

If equation (9) is applied to a greater-than-N-mode system, the measured inertances $\{I_{jk}(\omega)\}$ will each contain contributions from modes beyond the Nth and therefore the calculated modal constants will have errors associated with such out-of-range contributions. These errors can be reduced by increasing N. The effect is illustrated in Figure 3,

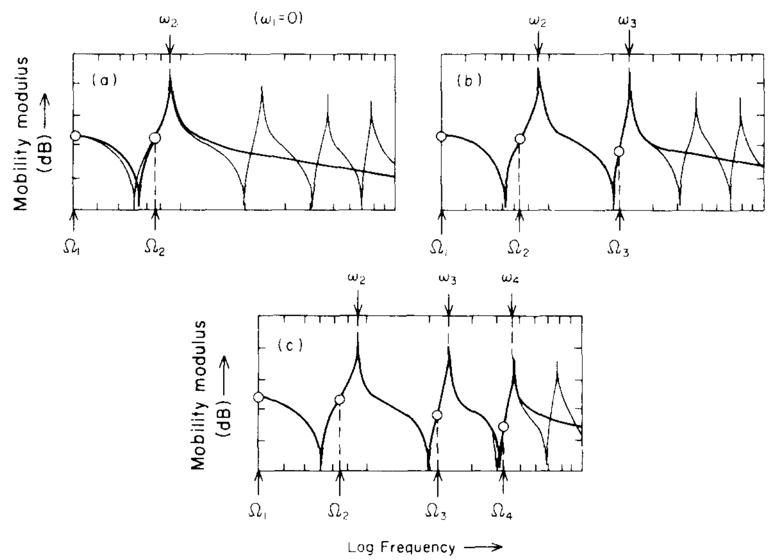

Figure 3. Comparison of regenerated curve with original data: incomplete modal representation. ——, True curve; ——, regenerated curve. (a) Two modes; (b) three modes; (c) four modes.

in which the tip mobility of a freely supported beam is represented by 2-, 3- and 4-mode approximations successively. Since the first mode of the body is at zero frequency, it is not shown on the plot although it is included in the model. Further consideration of responses of the same beam is given in subsequent figures. The circles on Figure 3 indicate the N selected responses used in identification calculations: in this case they are mid-amplitude responses below resonance. The regenerated curve, of course, passes through the selected data points and fits approximately elsewhere—clearly, the fit improves as the number of modes included increases. Above the last mode represented, the regenerated curve is always asymptotic to a line at -20 dB/decade. The fit of the two curves is quite good up to the last resonance included, but not beyond.

With an incomplete modal representation such as shown in Figure 3, there can be no unique solution for equation (9): the values obtained for the modal constants depend on the selection of response data. For this reason, a least-squares or pseudo-inverse approach, in which many sets of response data are used instead of only N, will not necessarily converge to give an optimum set of modal constants, and it is appropriate to consider which are the best points to select.

One may define those modes which have natural frequencies within the measured range as "low" and those of higher frequency outside the range as "high". Accordingly, one can designate the inertance contribution from low modes as I_L and that from high modes as I_H. Thus the measured inertances selected for the identification calculation are given by

$$\{I\} = \{I_L\} + \{I_H\}. \tag{12}$$

The modal constants $\{A\}$ obtained by use of equation (9) thus have two components,

$$\{A\} = \{A_C\} + \{A_E\}, \tag{13}$$

where the suffix C = Correct and E = Erroneous. It follows that

$$\{A_C\} = [R]^{-1}\{I_L\}, \qquad \{A_E\} = [R]^{-1}\{I_H\}. \tag{14, 15}$$

One should select response frequencies so as to maximize $\{A_C\}$ and minimize $\{A_E\}$, which is seen from equations (14) and (15) to be maximizing $\{I_L\}$ and minimizing $\{I_H\}$. It is also desirable for the elements of $[R]^{-1}$ to diminish along the rows so that less weight is given to the higher frequency inertance values which are more likely to be in error than those at low frequency because of the increasing influence of out-of-range modes.

The choice of response data points can have a very significant influence in the results, as shown in Figure 4. The response data of Figure 4(a) were chosen to have mobilities with mid-range moduli and +90° phase. The curve fit between regenerated and original data is reasonable, showing divergence only at higher frequencies. The response data of Figure 4(b) are substantially the same as for Figure 4(a), with the difference that the response at 50 Hz is omitted and one at 1000 Hz added. The regenerated curve based on identified modal constants in this case does indeed match the selected data points in amplitude and phase, but is otherwise drastically wrong. All the identified modal constants have the wrong sign, as indicated in Figure 4(b). Such a failure of identification is immediately obvious because of the mismatch of regenerated and original data. In this particular example the response frequencies Ω_1 to Ω_N are not evenly interspersed between the natural frequencies ω_1 to ω_N with the result that the $[R]^{-1}$ matrix features terms getting larger to the right along the rows so that the erroneous contribution of out-of-range high frequency modes is emphasized.

Such errors can be reduced by selecting response frequencies as far as possible at or just below *antiresonances* so as to minimize the contribution of out-of-range modes.

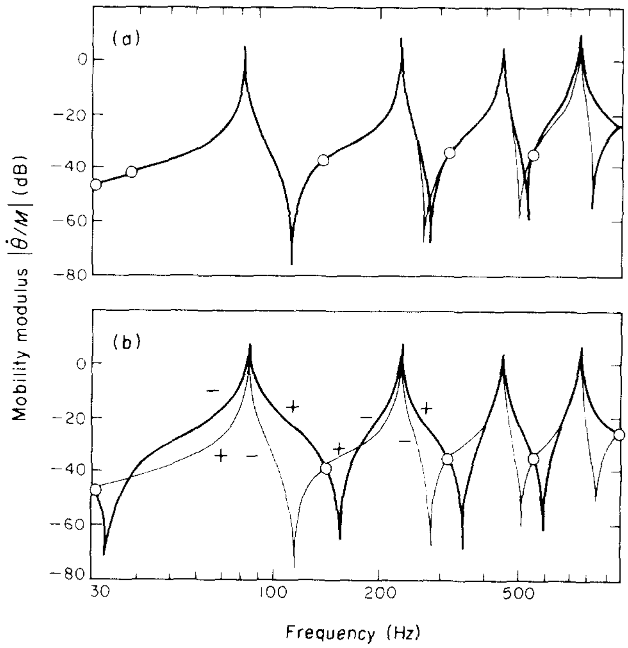

Figure 4. The effect of selection of response data upon the identification. ——, True curve; —— regenerated curve based on identified modal constants. (a) Selected response data at 31·6, 50·1, 144·5, 331, 575 Hz, resonances at 0, 85·9, 237, 464, 767 Hz; (b) selected response data at 31·6, 144·5, 331, 575, 1000 Hz, segments marked + have phase angle +90° and segments marked − have phase angle −90°.

Figure 5 shows the in- and out-of-range contributions for the rotational mobility at the tip of a beam. The measured antiresonances AR_1 to AR_5 (which incorporate the contributions of *all* modes) occur at frequencies lower than those of the summed in-range modes. At the measured antiresonances the contributions of in- and out-of-range modes are equal in amplitude, but of opposite sign. At frequencies below these antiresonances the contributions from the out-of-range modes are smaller than those in-range and the error in the identification calculation is reduced. Figure 6 is based on error-free inertance

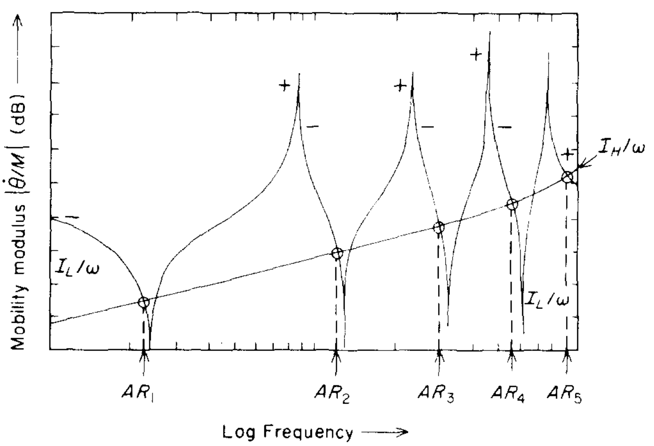

Figure 5. High and low frequency contributions to mobility. Segments marked + have phase +90°, those marked − have phase −90°.

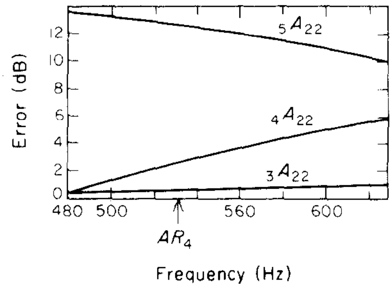

Figure 6. The effect of variation of a response data point in the vicinity of an antiresonance.

data and shows the errors of three of the five modal constants for a 5-mode approximation to an infinite-degree-of-freedom system. The figure shows that in the case of the modal constants of the third and fourth modes, choice of a data point below the fourth antiresonance reduces the error. The much larger error of the end-of-range 5th modal constant increases, however.

Experience has shown that satisfactory curve fits of regenerated data are usually obtained if the response data selected for identification contain as many antiresonances as possible. Antiresonances are, of course, associated with zeroes in $\{I\}$, thus reducing the effect of measurement errors in practical cases. An optimum selection of data used for identification of a point mobility is illustrated in Figure 7(a) in which only one non-zero response at low frequency is measured. The other data points—being antiresonances—are characterized only by their frequencies which contribute to matrix $[R]$.

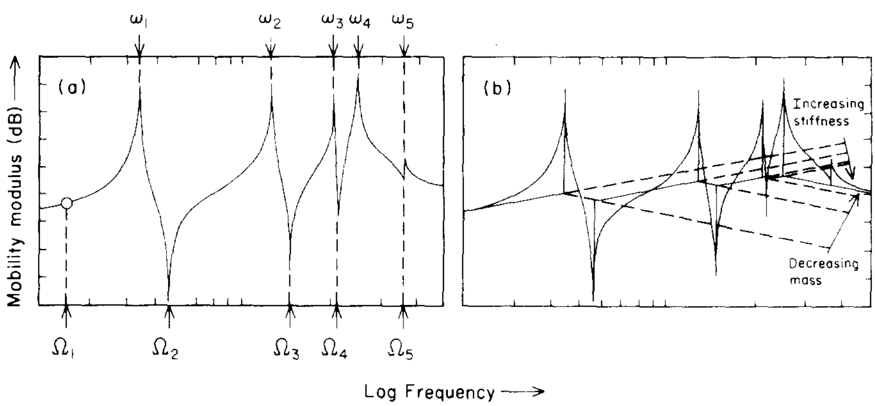

Figure 7. Identification of a point response: response data at antiresonances. (a) Point response identification; (b) Salter skeleton of point response.

The data used in these cases correspond very closely to those required for constructions of the Salter skeleton shown for the same point response in Figure 7(b). The skeleton is located by a stiffness line asymptotic to the true curve at low frequency and thereafter established by mass and stiffness lines intersecting at the frequencies of resonance and antiresonance.

A transfer response of the same 5-mode system is shown in Figure 8(a). Response data suitable for identification are indicated. In this case there are only two antiresonances, so three non-zero points were selected, two being at local minima. The alternation of modal constant signs is indicated.

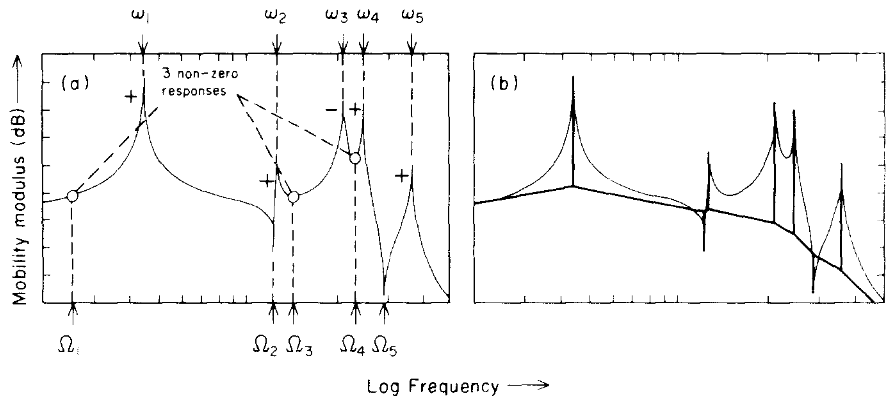

Figure 8. Identification of a transfer response: response data at antiresonances where possible. (a) Transfer response identification; (b) Salter skeleton of transfer response.

The corresponding Salter skeleton is shown as Figure 8(b) and it is seen that in the absence of antiresonances the downward trend of response level with increasing frequency is accentuated. This is a significant feature of most transfer responses.

Salter indicated that the skeleton should have its vertical lines adjusted in length according to the resonant amplitude of the response curve and then be clothed by a curve whose sharpness is inversely related to the amount of damping which Salter expressed in terms of Q, the inverse of the loss factor η.

The important advantage of the identification process of equation (9) as applied here is that it establishes the modal constants without errors attributable to damping, since the response data which are chosen are remote from the regions of resonance where damping has most effect. In other identification processes, expecially those in which circle-fitting in the complex plane is used, one evaluates damping first and other modal constants as a function of modal damping subsequently.

3.3. THE IDENTIFICATION OF AN ISOLATED MODE—THE "WINDOW" METHOD

It is to be expected that end-of-range modes will have enhanced values because they will incorporate the effects of more distant modes. If three modes are selected from an N-mode response, an identification can be carried out by using (for a point response) one non-zero response and two antiresonances. The "middle" modal constant will have a calculated value reasonably close to its true value, whereas the two "outside" constants will have enhanced values. The situation is sketched in Figure 9. It is thus possible to identify an N-mode response by a series of 3-mode "windows", with all the "middle" constants retained together with the lowest and the highest, as sketched in Figure 10. Regenerated curves based on such constants have produced acceptably accurate fits to measured data. Since the calculations involve only 3×3 matrices, a hand-calculator will suffice.

3.4. IDENTIFICATION OF SMALL MODAL CONSTANTS

So far, the systems discussed have had well spaced natural frequencies and modal constants of the same order of magnitude. In a more general case it is likely that the point at which response is measured will be quite close to a node of at least one of the modes and, consequently, will have little response at that particular resonance. In such a case, that modal constant will be small and will be subject to a relatively large error. This error is unlikely to cause a mismatch of regenerated curve to original data, but will

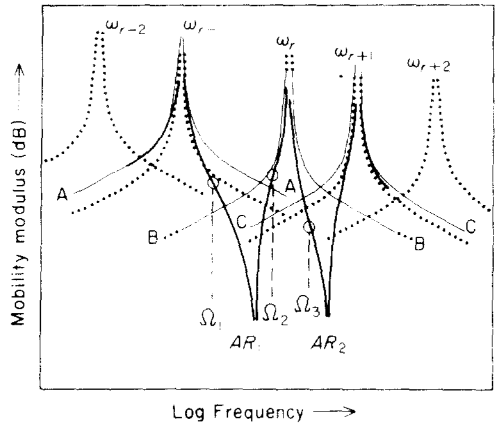

Figure 9. The identification of an isolated mode by the window method. · · · · , True responses of individual modes; ——, responses of modes identified in 3-mode calculation; ——, measured responses = true total of all modal contributions. Curve A = response of mode at ω_{r-1} raised to include effects of modes at ω_{r-2} and below; curve B = response of mode at ω_r maintained at true value; curve C = response of mode at ω_{r+1} raised to include effects of modes at ω_{r+2} and above.

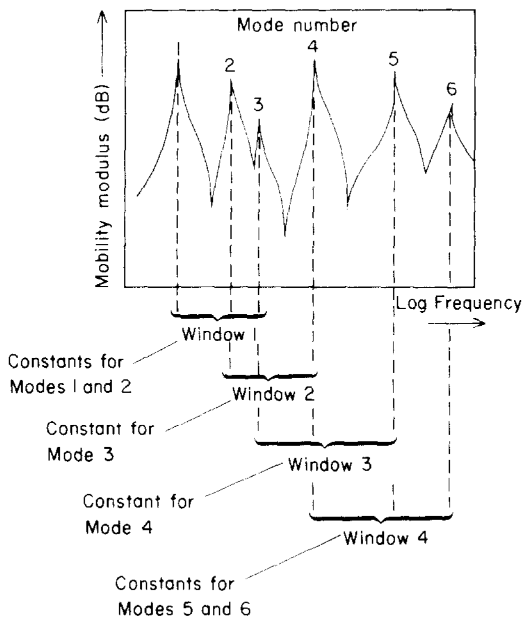

Figure 10. Illustration of the window method of identification.

be significant if it is used in the determining of a mode shape vector. This relationship of modal parameters is further discussed in section 4 below.

In the case of a weak isolated mode, the magnitude of the modal constant, A_R, is related to the ratio of the modal frequency ω_R to the adjacent antiresonance frequency ω_{AR}. Suppose that the local response is dominated by modes of lower frequency which have an effectively constant inertance, A_L, in the range of interest. Thus the inertance is given by

$$I = A_L + A_R/(1 - \omega_R^2/\omega^2). \qquad (16)$$

The local resonance occurs when $\omega = \omega_R$ and antiresonance when

$$A_L = -A_R/(1 - \omega_R^2/\omega_{AR}^2), \tag{17}$$

which leads to

$$A_R/A_L = (\omega_R/\omega_{AR})^2 - 1. \tag{18}$$

This relationship between modal constant and ω_R/ω_{AR} ratio is tabulated in Table 1. It follows that a weak mode will generally have an antiresonance very close to its resonance so that its effect will be simply to put a small local kink in the response curve, with no long-range effects.

When data from several response curves of the same system are compared, there are often small discrepancies in resonance frequencies, which are resolved by adjusting to the average value. In such a case, it is desirable to adjust the antiresonance frequency of a weak mode so as to preserve the (ω_R/ω_{AR}) ratio thereby avoiding gross error in the identified value of its modal constant.

TABLE 1

Small modal constant vs. (ω_R/ω_{AR}) ratio

(ω_R/ω_{AR}) ratio	0·95	0·98	0·99	1·01	1·02	1·05
Modal constant ratio	−0·1	−0·04	−0·02	+0·02	+0·04	+0·1

3.5. RESIDUALS

The idea of an isolated mode can usefully be extended to the consideration of an isolated group of modes. Suppose that the N modes of equation (5) were such a group, filling the frequency range of interest, but that there were also other modes outside this range at lower and higher frequencies. For the lower natural frequencies the inequality

$$\omega_r \ll \omega \tag{19}$$

would hold and in the range of interest, the L lower modes would be approximated by

$$\sum_{r=1}^{L} \frac{{}_rA_{jk}}{-\omega^2} = \frac{S_{jk}}{\omega^2}. \tag{20}$$

Conversely, for the higher natural frequencies one has

$$\omega_r \gg \omega \tag{21}$$

and the H higher modes are approximated by

$$\sum_{r=N+L+1}^{H} \frac{{}_rA_{jk}}{\omega_r^2} = R_{jk}. \tag{22}$$

The term $(-S_{jk}/\omega^2)$ corresponds to a mass residual which accounts for out-of-range low frequency terms. The name "samm" has been proposed for S_{jk}, which has dimensions of 1/mass and units of (1/kg).

The term (R_{jk}) corresponds to a residual flexibility accounting for the out-of-range high frequency terms. R_{jk} has dimension 1/stiffness. Equation (5) may now be rewritten as

$$\alpha_{jk}(\omega) = -\frac{S_{jk}}{\omega^2} + \sum_{r=L+1}^{N+L} \frac{{}_rA_{jk}}{\omega_r^2[1-(\omega/\omega_r)^2 + \mathrm{i}\eta_r]} + R_{jk}. \tag{23}$$

3.5.1. *Low frequency residuals*

It is possible to take account of low frequency residuals by including an arbitrary resonance frequency, lower than the range of interest, in identification calculations. In the case of freely supported structures or components, the low frequency response is dominated by the rigid body modes at zero frequency and the identification can be carried out by using equation (9) without modification. Only one zero frequency modal constant can be calculated by this method and this will generally contain contributions from more than one rigid body mode.

3.5.2. *High frequency residuals*

Although in many practical cases only *one* low frequency resonance (zero) need be considered, there is no such simplification in the case of high frequency residuals, since for a practical continuous structure, there is no bound to the number of modes. Representation of such modes is necessarily approximate, but equation (22) provides the key. The high frequency residual can be calculated by declaring an extra mode at an arbitrary frequency, ω_N, higher than the range of interest, and then using equation (9) in the normal way. The residual stiffness would be given by

$$K_{\text{res}} = 1/R_{jk} = \omega_N^2/{}_NA_{jk}. \tag{24}$$

The choice of ω_N has some influence on the accuracy of the modal constants within the range of interest as can be seen, for example, in Figure 11, which applies to the

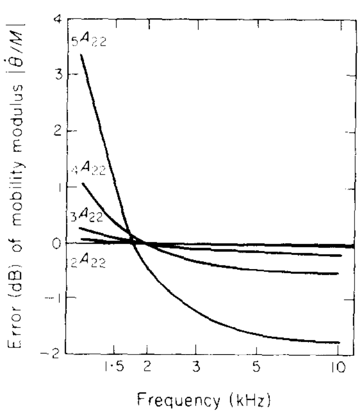

Figure 11. Sensitivity of modal constants to residual "resonance" frequency.

rotational response at a beam tip featured in Figures 5 and 6. The curves start at the true 6th natural frequency of the beam. Each applies to a different modal constant and each passes through zero error at some value of ω_6. A trial-and-error process of varying ω_6 and comparing the resulting regenerated response data with original data would give an optimum value in the range 1500–2000 Hz. Another feature of the curves is of value, however: they all become asymptotic to horizontal lines at the highest frequencies. Thus, if a high enough value of ω_6 is chosen, a definite set of modal constants will be established so that in equation (24), the high frequency residual can be expressed as a residual stiffness.

The discussion and example above correspond to the case of a point response for which force input and response occur at the same co-ordinate. It is usual in the case of *transfer* responses for the high frequency residual term to be negligibly small, as indicated by the steep fall of response in Figure 8 at higher frequencies.

3.5.3. *Visualization of high frequency residual*

Assuming that the low frequency residual S_{jj}/ω^2 can be represented by a zero-frequency mode, one may write, for the *point* receptance,

$$\alpha_{jj}(\omega) = \sum_{r=1}^{N} \frac{{}_rA_{jj}}{\omega_r^2[1-(\omega/\omega_r)^2 + \mathrm{i}\eta_r]} + R_{jj}. \tag{25}$$

Remembering equation (24), one can visualize the high frequency residual as a spring as illustrated in Figure 12.

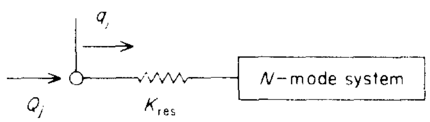

Figure 12. Visualization of high frequency residual as a spring.

4. RELATIONSHIPS OF MODAL PARAMETERS

4.1. DERIVATION OF MODAL CONSTANTS

Each of the co-ordinates of an N-degree-of-freedom system may have (in principle) an input force and each will have an acceleration response. Such a system will have a complete inertance matrix $[I(\omega)]_{N\times N}$, of which $I_{jk}(\omega)$, as defined in equation (6), is a typical element. For each mode there is a matrix $[A]_r$ containing all the modal constants of that mode. Their inter-relationship can be developed by extending equation (2) to include all j and k:

$$\{\phi\}_r\{\phi\}_r^{\mathrm{T}} = \begin{Bmatrix} {}_r\phi_1 \\ \vdots \\ {}_r\phi_N \end{Bmatrix} \{{}_r\phi_1 \cdots {}_r\phi_N\} = \begin{bmatrix} {}_r\phi_1^2 & ({}_r\phi_1\,{}_r\phi_2) & \cdots \\ \cdot & {}_r\phi_2^2 & \cdots \\ \cdot & \cdot & \cdots \\ \cdot & \cdot & {}_r\phi_N^2 \end{bmatrix} = \begin{bmatrix} {}_rA_{11} & {}_rA_{12} & \cdots \\ \cdot & {}_rA_{22} & \cdots \\ \cdot & \cdot & \cdots \\ \cdot & \cdot & {}_rA_{NN} \end{bmatrix} = [A]_r. \tag{26}$$

This equation can be used in the calculation of mode shape data $\{\phi\}_r$ from the identified modal constants $[A]_r$. It is not necessary to know all the elements of $[A]_r$ in order to find all the elements of $\{\phi\}_r$; one row or column will suffice.

For example, if the jth column of $[A]_r$ has been established by identifying the frequency response curves obtained at all N co-ordinates when a single force was applied at co-ordinate j, one can write

$${}_rA_{jj} = ({}_r\phi_j)^2, \quad \text{hence} \quad {}_r\phi_j = \pm({}_rA_{jj})^{1/2}, \tag{27}$$

$${}_rA_{jk} = {}_r\phi_j\,{}_r\phi_k, \quad \text{hence} \quad {}_r\phi_k = {}_rA_{jk}/{}_r\phi_j = {}_rA_{jk}/({}_rA_{jj})^{1/2}. \tag{28}$$

Equation (28) can be applied for $k = 1, (j-1)$ and $k = (j+1), N$ giving eventually all the data for $\{\phi\}_r$. Subsequently, the complete matrix of modal constants $[A]_r$ can be calculated from $\{\phi\}_r$ by using equation (26).

For one specific modal constant,

$$ {}_rA_{jk} = {}_r\phi_j\,{}_r\phi_k = [{}_rA_{ji}/({}_rA_{ii})^{1/2}][{}_rA_{ki}/({}_rA_{ii})^{1/2}] = {}_rA_{ji}\,{}_rA_{ki}/{}_rA_{ii}. \tag{29} $$

Thus, the modal constants of the response at co-ordinate j arising from force at co-ordinate k can be *derived* from the modal constants of responses at i, j and k arising from force input at a *different* co-ordinate, i.

4.2. APPLICATION OF DERIVATION RELATIONSHIPS

4.2.1. *Single point excitation*

The possibility of determining a complete mode shape vector $\{\phi\}_r$ from measurements of response obtained with a single co-ordinate of excitation has been exploited by several investigators, including Flanelly *et al.* [7, 8], Goyder [3] and Potter and Richardson [9], and may now be regarded as a standard technique. The derivation of one row or column of $[A]_r$ involves identification of one point response and $(N-1)$ transfer responses. It is to be expected in practice that some transfer measurements relating to points of a structure remote from each other or otherwise poorly coupled (by proximity to a node, for example) will give modal constants of small value which have proportionately large errors.

Richardson and Kniskern [10] have responded to these difficulties by proposing a method which allows the inclusion of data from several columns or rows of the modal constant matrix: in other words, by using more than one excitation point.

4.2.2. *Multiple point measurements*

A method of acquiring more reliable data is to obtain the *point* modal constants corresponding to the main diagonal of $[A]_r$ by identifying the point responses obtained at each co-ordinate in turn. It will be remembered that point responses always feature antiresonances and have levels of response which tend to be maintained, rather than fall off, at higher frequencies. These features enhance the likelihood of obtaining accurate modal constants. The *numerical* values of the elements of the mode shape matrix $[\phi]$ are simply obtained from the square roots of the corresponding modal constants, as in equation (27). These square roots are indeterminate in sign, and thus it is necessary to obtain the signs by other means. This is done most readily by measuring the transfer responses associated with force input at *one* co-ordinate which is not a node of any mode and finding the *signs* of the modal constants from the phase information.

4.2.3. *Point response at inaccessible locations*

Some points on structures are accessible for attachment of accelerometers, but not accessible for force input, requiring as it does not only the force transducer but also alignment of a shaker and drive rod. The inside of a small diameter bearing housing would typify such an inaccessible location. The point inertance is required, perhaps, in order to predict the effect of the support upon the dynamics of a rotating shaft. If one designates the inaccessible location as co-ordinate A and nearby accessible location as co-ordinate B, the inertance matrix relating A and B is

$$ [I] = \begin{bmatrix} I_{AA} & I_{AB} \\ I_{BA} & I_{BB} \end{bmatrix}. \tag{30} $$

The elements of the second column, I_{AB} and I_{BB}, with force input at B, can be measured. The modal constants, ${}_rA_{AB}$ and ${}_rA_{BB}$, can be identified and then ${}_rA_{AA}$ found, by using the equation

$$ {}_rA_{AA} = {}_rA_{AB}^2 / {}_rA_{BB}. \tag{31} $$

The response I_{AA} can then be reconstituted by using a sum of modal contributions similar to equation (5). However, difficulties arise if there are residual terms, as discussed in section 4.3, and a discussion of the associated problem is given in reference [11].

4.2.4. *Improvement of rotational measured data*

Some practical difficulties have been encountered in the measurement of rotational mobilities of beams. For example, the inertance matrix for the tip of a beam can be written as

$$ [I] = \begin{bmatrix} (\ddot{X}/F) & (\ddot{X}/M) \\ (\ddot{\theta}/F) & (\ddot{\theta}/M) \end{bmatrix}. \tag{32} $$

The parameter $(\ddot{\theta}/M)$ is difficult to measure accurately, not least because of the problem of producing an input moment, M. As is explained in what follows, inaccuracies in $(\ddot{\theta}/M)$ may be compensated for by deriving the modal constants of that parameter from those of $(\ddot{X}/F)$ and $(\ddot{\theta}/F)$ which are amenable to reasonably accurate measurement.

4.3. RESIDUALS AND DERIVATION

It must now be pointed out that high frequency residuals cannot be derived. Derivation is possible for modes within the frequency range of interest because it is an expression of the orthogonality properties of the normal mode. If a mode shape is known and the amplitude of *one* particular element of that mode is known, then the amplitudes of *all* elements are determined. The high frequency residual is an approximation to the combined effect of a number of modes and can be expressed in terms of a modal constant of a fictitious mode at an assumed "resonance" frequency. *There is no residual mode shape.* Consequently, residual terms for I_{AA} cannot be derived from I_{AB}, I_{BB} measurements. At this juncture, it seems as if the use of a high frequency residual and derivation—two most useful devices in modal identification—nullify each other. Fortunately, there is a workable solution to the problem: the representation of a high frequency residual as a spring introduced above in section 3.5 proves to be a valuable contrivance [12].

Similar comments apply in general to low frequency residuals in those cases where the effects of several modes of different frequencies are included. The most common cases encountered in this study of lightly damped structures is of freely supported components. Their low frequency residuals correspond to rigid body modes at zero frequency, to be dealt with in the next section.

4.4. RIGID BODY MODES

A freely supported body has six rigid body modes. Three of these are translational and three are rotational and each has a mode shape which is orthogonal to all the others. Since they all have the same resonance frequency, zero, they can combine. A general rigid body motion is thus a combination of rigid body modes. As in the case of bending modes, the individual rigid body modes have definite shapes which relate to specific co-ordinates and are amenable to the derivation process. It is very easy to excite rigid body motion featuring more than one mode and in such a case, derivation is not simple and can only work when the modes are separated. It is a feature of the identification calculations based on equation (8), which are used in the computer program, that $[R]$ is singular if two resonance frequencies are the same. Consequently, the program can identify only *one* set of modal constants at zero frequency—most usually corresponding to a *combination* of modes—and these must be separated before $[\Phi]$, the mode shape matrix, can be evaluated. The motion of a beam in two dimensions is a simple case which will be discussed here.

4.4.1. *Separation of rigid body modes*

Consider the tip response of a beam as shown in Figure 13, with inertance matrix

$$[I(\omega)] = \begin{bmatrix} (\ddot{X}/F) & (\ddot{X}/M) \\ (\ddot{\theta}/F) & (\ddot{\theta}/M) \end{bmatrix}. \tag{33}$$

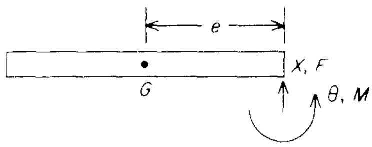

Figure 13. Rigid body tip responses of a free–free beam.

One wishes to find the modal constants of the rigid body modes, ${}_0[A]$, and this process is facilitated by use of equation (8). First, one sets $\omega_1 = 0$ and observes that the first column of $[R]$ has each element unity. Then one observes that the remaining elements of the first row of $[R]$ tend to zero as Ω_1, the first excitation frequency, tends to zero. Thus, one obtains:

$$I_{jk}(0) = {}_0A_{jk}, \tag{34}$$

where the prefix $_0$ denotes first mode (at zero frequency). The elements of ${}_0[A]$ can thus be found from consideration of low frequency inertances which relate steady accelerations to steady forces.

There are in fact two rigid body modes excited by an input force F which does not pass through the centroid G and which consequently produces rotation about G as well as translation of G. Thus

$$Fe = I_G\ddot{\theta}, \qquad F = m\ddot{X}_T, \tag{35, 36}$$

where $\ddot{X}_T$ is the component of $\ddot{X}$ which corresponds to the translational rigid body mode. The rotational component $\ddot{X}_R$ is given by

$$\ddot{X}_R = e\ddot{\theta} = e^2F/I_G, \tag{37}$$

upon using equation (35). Combining equations (36) and (37) and rearranging gives

$$\ddot{X}/F = (\ddot{X}_T + \ddot{X}_R)/F = (1/m) + (e^2/I_G) = {}_0A_{11}, \tag{38}$$

and, from equation (35),

$$(\ddot{\theta}/F) = e/I_G = {}_0A_{21}. \tag{39}$$

The applied moment M excites only the rotational rigid body mode:

$$M = I_G\ddot{\theta}. \tag{40}$$

Thus

$$(\ddot{\theta}/M) = 1/I_G = {}_0A_{22}, \tag{41}$$

and using equation (37) again gives

$$(\ddot{X}_R/M) = e/I_G = {}_0A_{12}. \tag{42}$$

The complete matrix of modal constants is

$$ {}_0[A] = \begin{bmatrix} {}_0A_{11} & {}_0A_{12} \\ {}_0A_{21} & {}_0A_{22} \end{bmatrix} = \begin{bmatrix} (1/m + e/I_G) & e/I_G \\ e/I_G & 1/I_G \end{bmatrix}. \tag{43} $$

Simple application of the derivation formula (by which $(\ddot{\theta}/M)$ is obtained in terms of $(\ddot{X}/F)$ and $(\ddot{\theta}/F)$) does not hold, since

$$ {}_0A_{22} \neq {}_0A_{21}^2 / {}_0A_{11}. \tag{44} $$

This happens because the two rigid body modes which are excited by F are not separated. When the separation has been carried out, by calculating the mass of the free body and simply subtracting its reciprocal, one may write

$$ {}_0[A]_T = \frac{1}{m}\begin{bmatrix} 1 & 0 \\ 0 & 0 \end{bmatrix} = \frac{1}{m}\begin{Bmatrix} 1 \\ 0 \end{Bmatrix}\{1 \quad 0\}, \qquad {}_0[A]_R = \frac{1}{I_G}\begin{bmatrix} e^2 & e \\ e & 1 \end{bmatrix} = \frac{1}{I_G}\begin{Bmatrix} e \\ 1 \end{Bmatrix}\{e \quad 1\}, \tag{45, 46} $$

$$ {}_0[A] = {}_0[A]_T + {}_0[A]_R. \tag{47} $$

Now that the sets of modal constants have been separated, useful derivation relationships *do* hold:

$$ {}_0A_{22T} = {}_0A_{21T}^2 / {}_0A_{11T}, \qquad {}_0A_{22R} = {}_0A_{21R}^2 / {}_0A_{11R}. \tag{48, 49} $$

When selected curves from the response surface of a freely–supported body are identified, it is the total matrix ${}_0[A]$ which is obtained, and in the general case it might be quite difficult to separate the modal constants of several rigid body modes although the general relationships involved in rigid body motion have been developed [12].

4.5. CONSISTENCY

It is usually possible to collect more data than is strictly necessary for identifying the modal constants of a system. Such "redundant" data can be used to make second estimates of constants and thus help to avoid gross errors. Suppose that one column *and* the leading diagonal of a mobility or inertance matrix have been measured, a procedure which is likely to give the best data for identification as discussed in section 4.1. There will have been N points of excitation used and the first step to obtaining a consistent model is to check that the resonance frequencies measured at different points do coincide, or, if not, to estimate a best value by using simple averaging. It is important that the identification calculations for the different point responses are all carried out with the *same* set of nominal resonance frequencies, care being taken with adjacent antiresonance frequencies as indicated above, in section 3.4.

It is to be expected that the point modal constants will be the more accurately evaluated. Extra data will be available from a set of transfer responses which will give second estimates for the point modal constants using the derivation relationships developed in section 4.1. In some cases, particularly where rotations are concerned, the derived values of point modal constants may well be nearer their true values than the directly identified set. In any event, the values ultimately adopted for the matrices of modal constants $[A]_r$ must be adjusted so that they consistently conform to the derivation relationships of equation (29).

The data contained in the N matrices, designated $[A]_r$, can be reduced and be contained in the single matrix $[\Phi]_{N\times N}$. The resonance frequencies will be listed (squared) in the diagonal matrix $[\omega_r^2]_{N\times N}$.

Sometimes, the application of consistency checks to redundant measurements yields an unsatisfactory result: namely, that consistency is clearly not observed by the data.

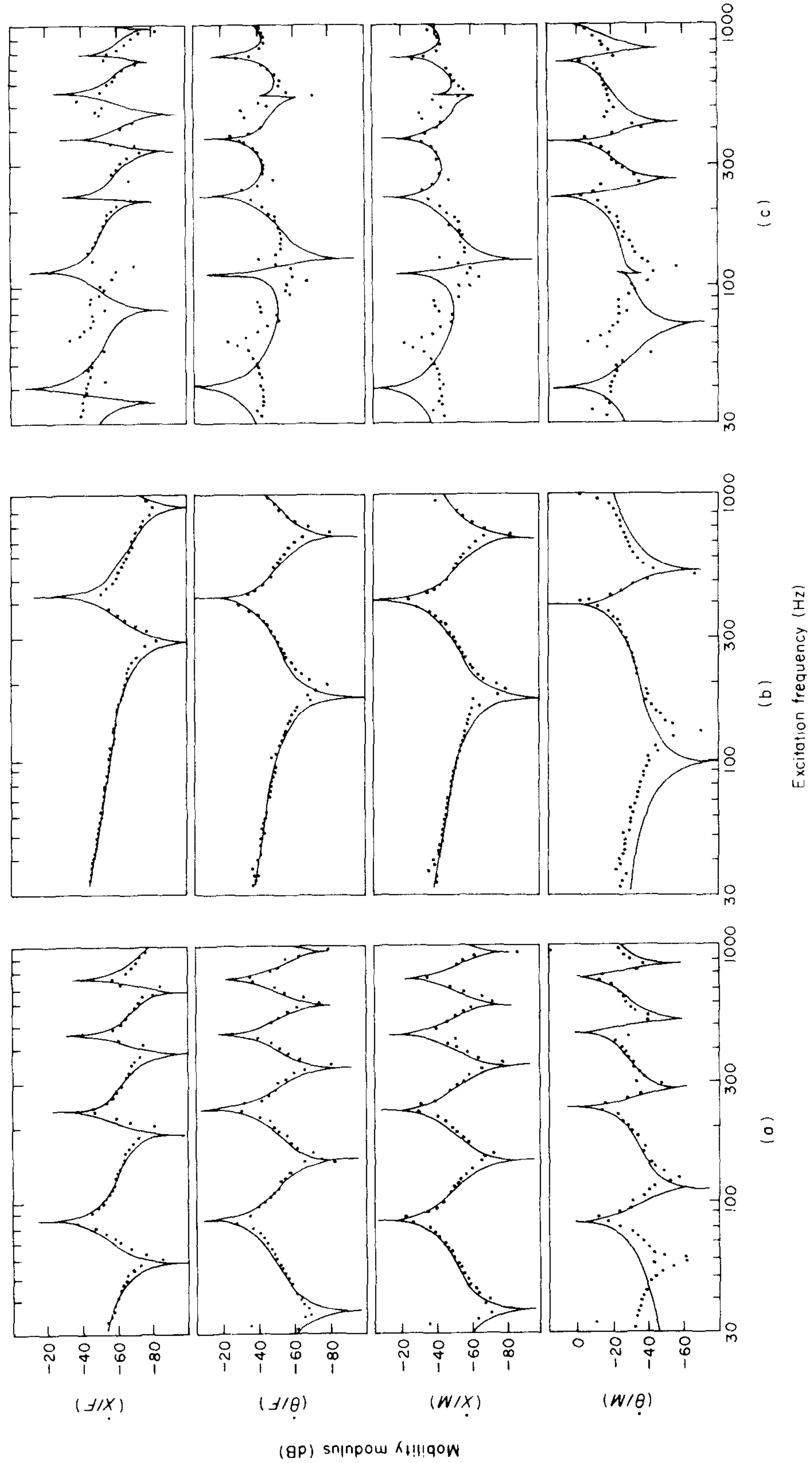
Mobility modulus (dB)
(Ẋ/F)
(θ̇/F)
(Ẋ/M)
(θ̇/M)
Excitation frequency (Hz)
(a)
(b)
(c)
30
100
300
1000

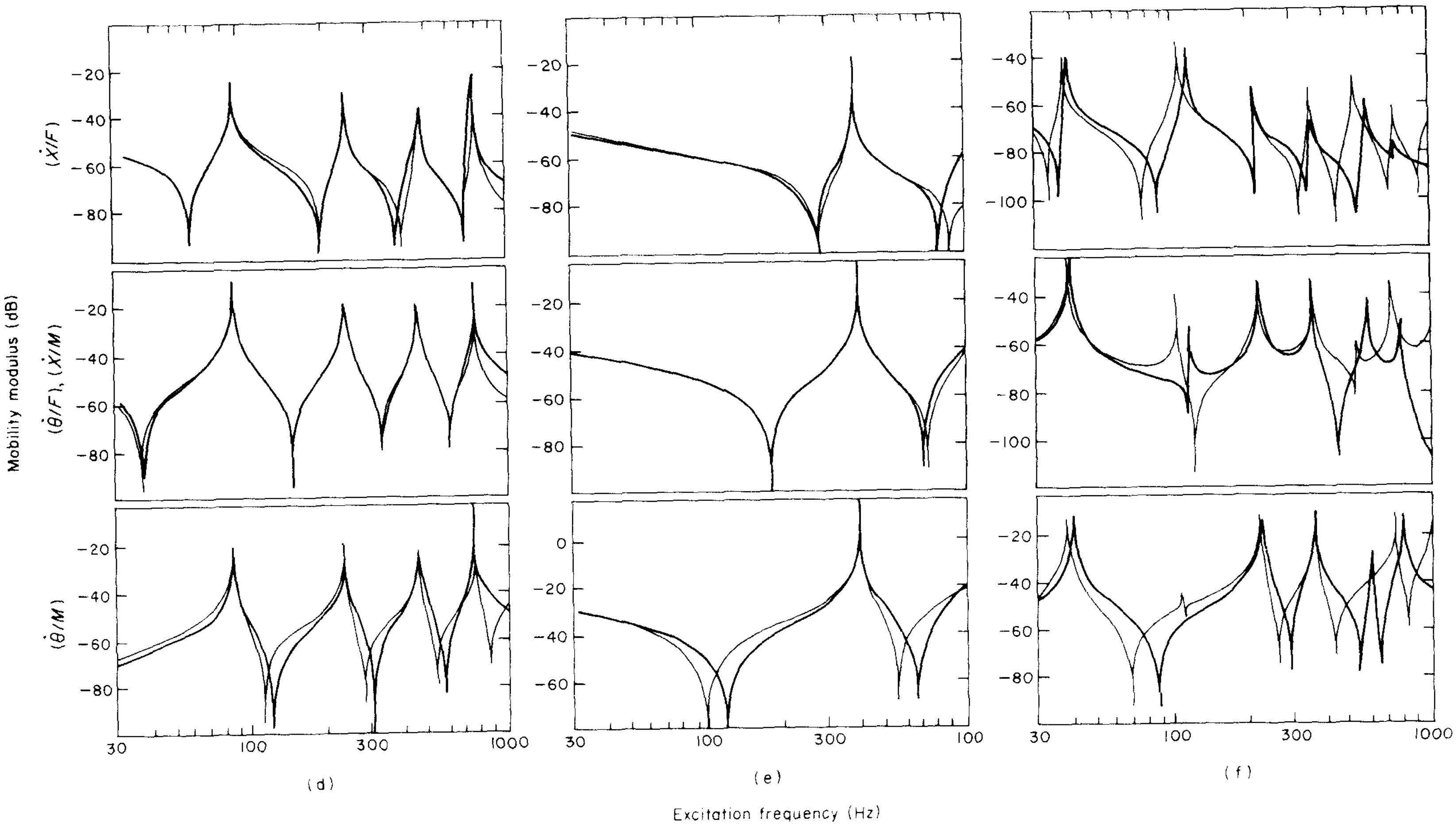

Figure 14. Mobility properties. (a) Long Beam I: ——, theoretical; · · · ·, direct measurements. (b) Short Beam I: key as for (a). (c) Coupled Beam I: ——, theoretical; · · · ·, predicted from direct measurements on component beams. (d) Long Beam II: ——, theoretical; ——, smoothed measurements for $(\dot{X}/F)$, $(\dot{X}/M)$, and derived measurements for $(\dot{\theta}/F)$, $(\dot{\theta}/M)$. (e) Short Beam II: key as for (d). (f) Coupled Beam II: ——, theoretical; ——, predicted from smoothed/derived measurements on component beams.

This can arise for a number of reasons; one, clearly, is that the measured data used are very inaccurate but a second one of particular interest is the possibility that what has been identified as a single mode resonance is in fact a number of modes whose frequencies are so close that they cannot be seen separately. Such conditions arise on any system with two or more *identical* natural frequencies, and in practical structures with close natural frequencies where the prevailing damping level is just sufficient to merge the two modes into a single resonance peak. In these cases, it is not possible to identify the modal properties satisfactorily (one of the basic conditions of the method has been violated) but it is possible to detect the existence of a problem of this type and thus to avoid some of the consequences which might ensue from ignoring it altogether.

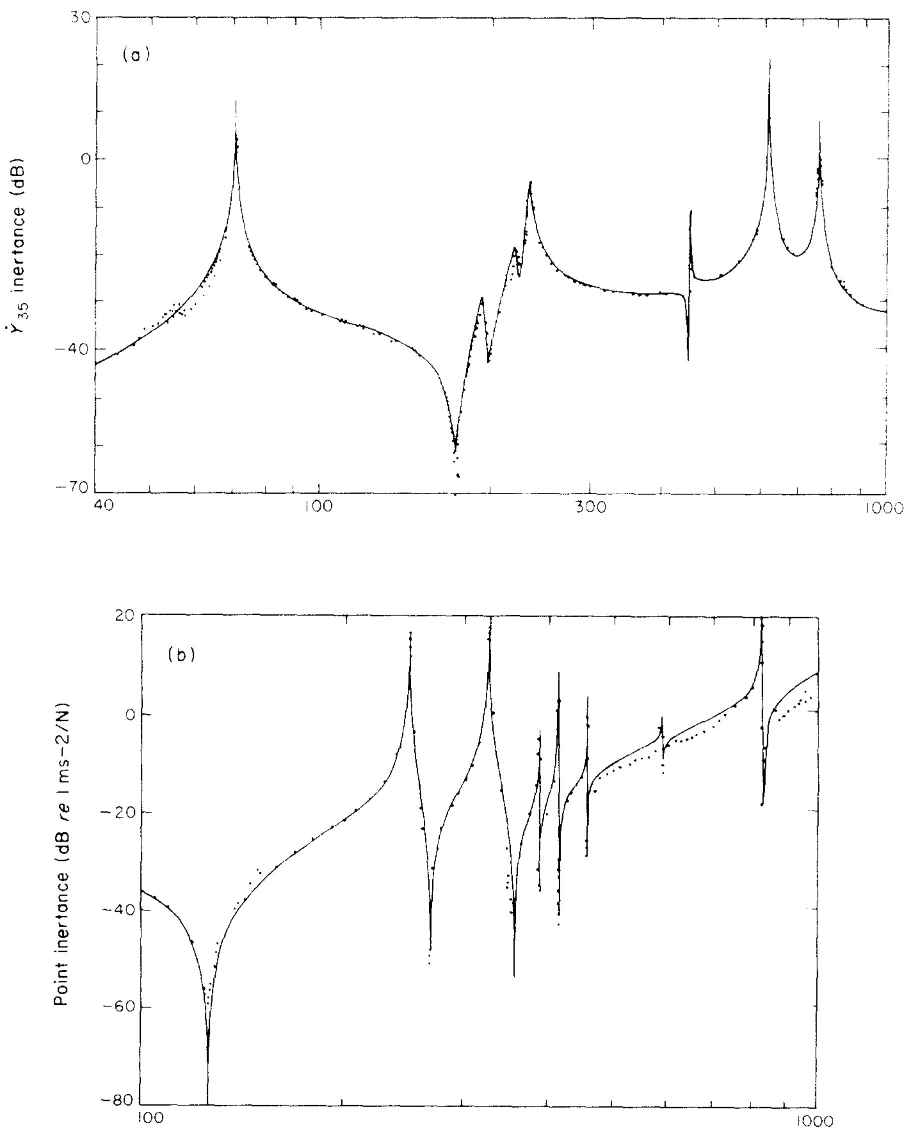

Figure 15. Measured and identified (a) transfer inertance of a compressor blade, (b) point inertance on a turbine-rotor and (c) mobility of helicopter platform. For (a) and (b), · · · · measured points and —— identified curve; for (c), · · · · measured points and —— regenerated curve.

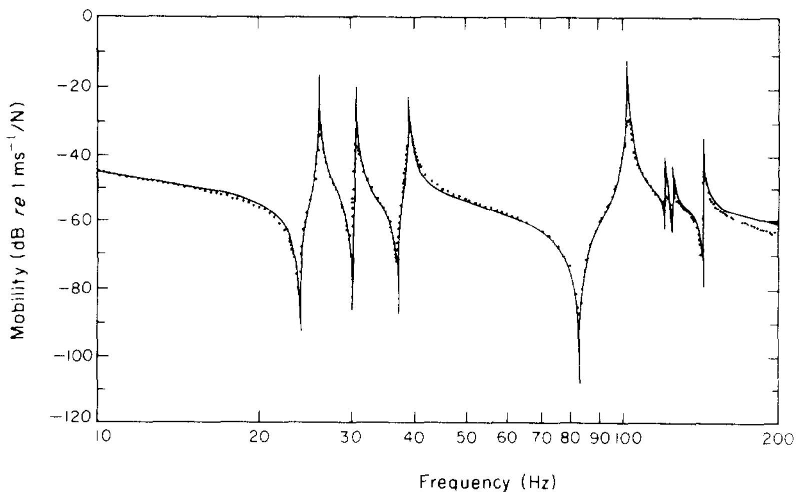

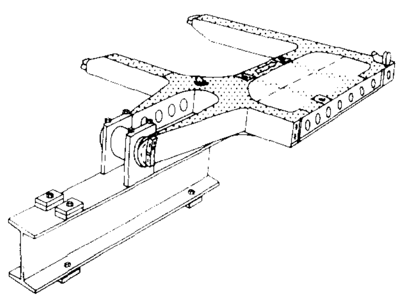

(c)

Fig. 15 (*contd.*)

5. APPLICATIONS OF THE IDENTIFICATION AND DERIVATION PROCESS

5.1. MEASUREMENTS ON BEAMS

Measurements were made of the point mobility matrices at the tips of two freely supported beams. The matrices involved co-ordinates of translation and of rotation as indicated in Figure 13. The beams were made of steel, with a cross-section 25 mm × 32 mm. The so-called "Long Beam" had length 1·4 m and natural frequencies at 0, 86, 237, 464, 767, etc., Hz. The "Short Beam", of length 0·65 m, had natural frequencies at 0, 399, 1100, etc., Hz—quite distinct from those of its companion.

The vibration behaviour of such simple beams is accurately predictable and the theoretical mobilities of the beams are plotted as continuous lines in Figures 14(a) and (b). Corresponding measured data are plotted as points and it can be seen that there are minor random discrepancies (as might be expected), but also some major systematic errors, most noticeably in the rotational mobility ($\dot{\theta}/M$) at low frequency.

The Long and Short Beams coupled end to end at a butt joint would together constitute a "Coupled Beam" of length 2·05 m, having natural frequencies 0, 40, 110, 217, 358, 535, 747, etc., Hz. The mobility properties at a point 0·65 m along the beam were calculated theoretically and are displayed as the continuous lines of Figure 14(c). The points on this figure were calculated, frequency by frequency, from the raw data of

Figures 13 and 14(a), by using standard mobility coupling matrix calculations. It is apparent that the correlation between these calculations and the ideal is very poor.

Identification calculations were carried out on the data for the individual beams, having the effect of smoothing the curves and eliminating random errors. Further calculations were then made so that the modal constants of the second row of the mobility matrix were derived from those calculated for the first row, due account being taken of the rigid body modes.

Thus, the relatively difficult-to-measure quantities, $(\dot{\theta}/F)$ and $(\dot{\theta}/M)$, were obtained from the inherently more easily measured $(\dot{X}/F)$ and $(\dot{X}/M)$. The results of the identification and derivation process on the two beams were shown as Figures 14(d) and (e), which show considerable improvement when compared with their predecessors, Figures 14(a) and (b), having no random errors and greatly reduced systematic errors. Finally, the resultant predicted mobilities of the nominated point on the Coupled Beam are shown in Figure 14(f). Discrepancies between the calculated result and the ideal are apparent, but the responses have the correct general characteristics and are certainly a significant improvement on the raw data predictions of Figure 14(c).

5.2. APPLICATIONS TO PRACTICAL STRUCTURES

In order to demonstrate the application of this identification method to practical structures, we cite three examples where it has been used on components of complex engineering structures. The three structures are as follows: (i) a compressor blade; (ii) a gas turbine rotor; (iii) an external carrier platform for a helicopter. In each case, a mathematical model of the component in question was required for further analysis—such as the vibration modelling of a larger structure of which the testpiece was a component [13], or the derivation of excitation forces [14]. Figure 15 illustrates a mobility plot for each of the components, showing both measured data (as points) and regenerated data (continuous line) and all share the characteristic that the inherent damping is so low as to inhibit detailed measurements on the resonant regions.

6. CONCLUDING REMARKS

In this paper we have presented a method for the experimental modal analysis of structures which is of particular value in those cases where the damping is so light that (a) its magnitude is of no intrinsic interest, and (b) accurate measurements of the resonant response characteristics are very difficult. Such conditions are frequently encountered in studies of practical systems where the separate components of a complex structural assembly are studied individually (usually to determine a suitable subsystem model which can then be combined with other similar models to describe the full assembly). In these cases, attention is generally confined to an undamped model—primarily to predict natural frequencies—since the actual damping levels of the full assembly will usually be dominated by the joints between the components, and not by the damping possessed by the components themselves.

Thus one can clearly identify a class of structure for which an accurate mass and stiffness description is required. One can also assert that when testing such components, it is often difficult to make accurate frequency response measurements in the immediate vicinity of the resonances—because of their low damping—and thus a technique such as the one reported here which does not rely on the accuracy of these data is of particular value.

The method has been used on many applications over a period of several years—both in the research laboratory and in industry—and has proven to be a robust and reliable tool, especially when used with engineering skill and judgement. Its simplicity makes it easy to implement and the reduced version—the "window" method—is amenable to hand-calculator programming for accurate estimation of an individual modal parameter.

As with all experimental modal analysis methods, it is recommended that some redundant frequency responses be measured and analyzed in order to provide cross checks of the accuracy of the modal parameters determined in this way. Visual comparison of experimental and theoretically regenerated data is not always a sufficiently critical assessment.

REFERENCES

1. J. P. SALTER 1969 *Steady State Vibration*. Havant, Hampshire: Mason Press.
2. D. R. GAUKROGER, K. H. HERON and C. W. SKINGLE 1974 *Journal of Sound and Vibration* **35**, 559–571. The processing of response data to obtain modal frequencies and damping ratios.
3. H. G. D. GOYDER 1976 *Institute of Sound and Vibration Research Technical Report No.* 87. Structural modelling by the curve fitting of measured frequency response data.
4. D. J. EWINS and J. KIRSHENBOIM 1982 (in preparation).
5. R. E. D. BISHOP and D. C. JOHNSON 1960 *The Mechanics of Vibration*. Cambridge University Press.
6. D. J. EWINS 1975 *Journal of Sound and Vibration* **43**, 595–605. Estimation of resonant peak amplitudes.
7. W. G. FLANNELLY and N. GIANSANTE 1974 *USAAMRDL-TR-*74-64, *Report Produced by Kaman Aerospace Corporation*. Experimental verification of system identification.
8. W. G. FLANNELLY, A. BERMAN and N. GIANSANTE 1972 *Kaman Aerospace Corporation USAAMRD Technical Report* 72-63*A Eustis Directorate U.S. Army Air Mobility Research and Development Laboratory, Fort Eustis, Virginia*. Research on structural dynamic testing by impedance methods, Volume I: Structural system identification from multipoint excitation.
9. R. POTTER and M. RICHARDSON 1974 *ISA Paper No.* 74-630. Mass stiffness and damping matrices from measured modal parameters.
10. M. RICHARDSON and J. KNISKERN 1974 *ISA/ASI* 74250 (239–246). Identifying modes of large structures of an elastic structure from measured transfer function data.
11. D. J. EWINS 1980 *Journal of Sound and Vibration* **70**, 69–75. On predicting point mobility plots from measurements of other mobility parameters.
12. P. T. GLEESON 1980 *Ph.D. Thesis, University of London*. Identification of spatial models.
13. D. J. EWINS, J. M. M. SILVA and G. MALECI 1980 *Shock and Vibration Bulletin* **50**, 155–170. Vibration analysis of a helicopter with an externally-attached carrier structure.
14. D. J. EWINS and B. HILLARY 1980 *Proceedings of Symposium on Aeroelasticity in Turbomachines, Lausanne*. A method for force determination from vibration response measurements.